Attenuation of yeast UPR is essential for survival and is mediated by *IRE1* kinase

Aditi Chawla,[1] Sutapa Chakrabarti,[2] Gourisankar Ghosh,[2] and Maho Niwa[1]

[1]Division of Biological Sciences, Section of Molecular Biology, and [2]Division of Chemistry and Biochemistry, University of California, San Diego, La Jolla, CA 92093

The unfolded protein response (UPR) activates Ire1, an endoplasmic reticulum (ER) resident transmembrane kinase and ribonuclease (RNase), in response to ER stress. We used an in vivo assay, in which disappearance of the UPR-induced spliced *HAC1* messenger ribonucleic acid (mRNA) correlates with the recovery of the ER protein-folding capacity, to investigate the attenuation of the UPR in yeast. We find that, once activated, spliced *HAC1* mRNA is sustained in cells expressing Ire1 carrying phosphomimetic mutations within the kinase activation loop, suggesting that dephosphorylation of Ire1 is an important step in RNase deactivation. Additionally, spliced *HAC1* mRNA is also sustained after UPR induction in cells expressing Ire1 with mutations in the conserved DFG kinase motif (D828A) or a conserved residue (F842) within the activation loop. The importance of proper Ire1 RNase attenuation is demonstrated by the inability of cells expressing Ire1-D828A to grow under ER stress. We propose that the activity of the Ire1 kinase domain plays a role in attenuating its RNase activity when ER function is recovered.

Introduction

In eukaryotic cells, folding and modification of nascent membrane and secreted proteins take place in the ER (Wickner and Schekman, 2005). The increased demand of the ER activates the unfolded protein response (UPR) (Kaufman, 1999; Mori, 2000; Patil and Walter, 2001; Harding and Ron, 2002; Ron and Walter, 2007). In yeast, the UPR is initiated by activation of the ER transmembrane sensor Ire1 (Cox et al., 1993; Mori et al., 1993), leading to Ire1 autophosphorylation and oligomerization (Shamu and Walter, 1996; Lee et al., 2008; Aragón et al., 2009) and activation of Ire1 endo-RNase. Ire1 RNase-mediated excision of the translation-inhibitory intron in *HAC1* mRNA is essential for the expression of the Hac1 protein (Cox and Walter, 1996; Sidrauski and Walter, 1997; Kawahara et al., 1998; Rüegsegger et al., 2001). The Hac1 protein, a UPR-specific transcription factor, then induces UPR target gene expression, including ER resident chaperones and critical protein-folding enzymes (Travers et al., 2000).

Although the initial phase of the UPR pathway has been well studied, subsequent events leading to the reestablishment of ER homeostasis and details of how UPR is finally attenuated have only been partially studied. Upon activation, the extent of Ire1 RNase activity must be tightly controlled as both ectopic expression of the spliced form of *HAC1* mRNA (Kawahara et al., 1997) and the overexpression of Ire1 cause cells to grow poorly, highlighting the importance of UPR attenuation. Here, we establish a UPR attenuation assay in vivo and find an important role for the Ire1 kinase domain in attenuating *HAC1* splicing beyond its known role in activation.

Results and discussion

To test the molecular steps involved in the recovery phase of the UPR, we profiled Ire1 activity by monitoring *HAC1* mRNA splicing upon UPR activation. Wild-type (WT) yeast cells were incubated with the well-characterized UPR inducer tunicamycin (Tm) for an extended length of time. Tm inhibits glycosylation in the ER, resulting in the accumulation of unglycosylated proteins, which leads to the activation of the UPR. Initially, spliced *HAC1* mRNA appeared upon Tm incubation (Fig. 1, A–I) as reported previously (Cox and Walter, 1996; Kawahara et al., 1998). Under the experimental conditions used, the presence of

Correspondence to Maho Niwa: niwa@ucsd.edu

Abbreviations used in this paper: BTPNA, *N*-benzoyl-L-tyrosine *p*-nitroanilide; CPY, carboxypeptidase Y; IRK, insulin receptor kinase; LKT, linker kinase tail; MANT, *N*-methylanthraniloyl nucleotide; Tm, tunicamycin; UPR, unfolded protein response; WT, wild type.

The Rockefeller University Press $30.00
J. Cell Biol. Vol. 193 No. 1 41–50
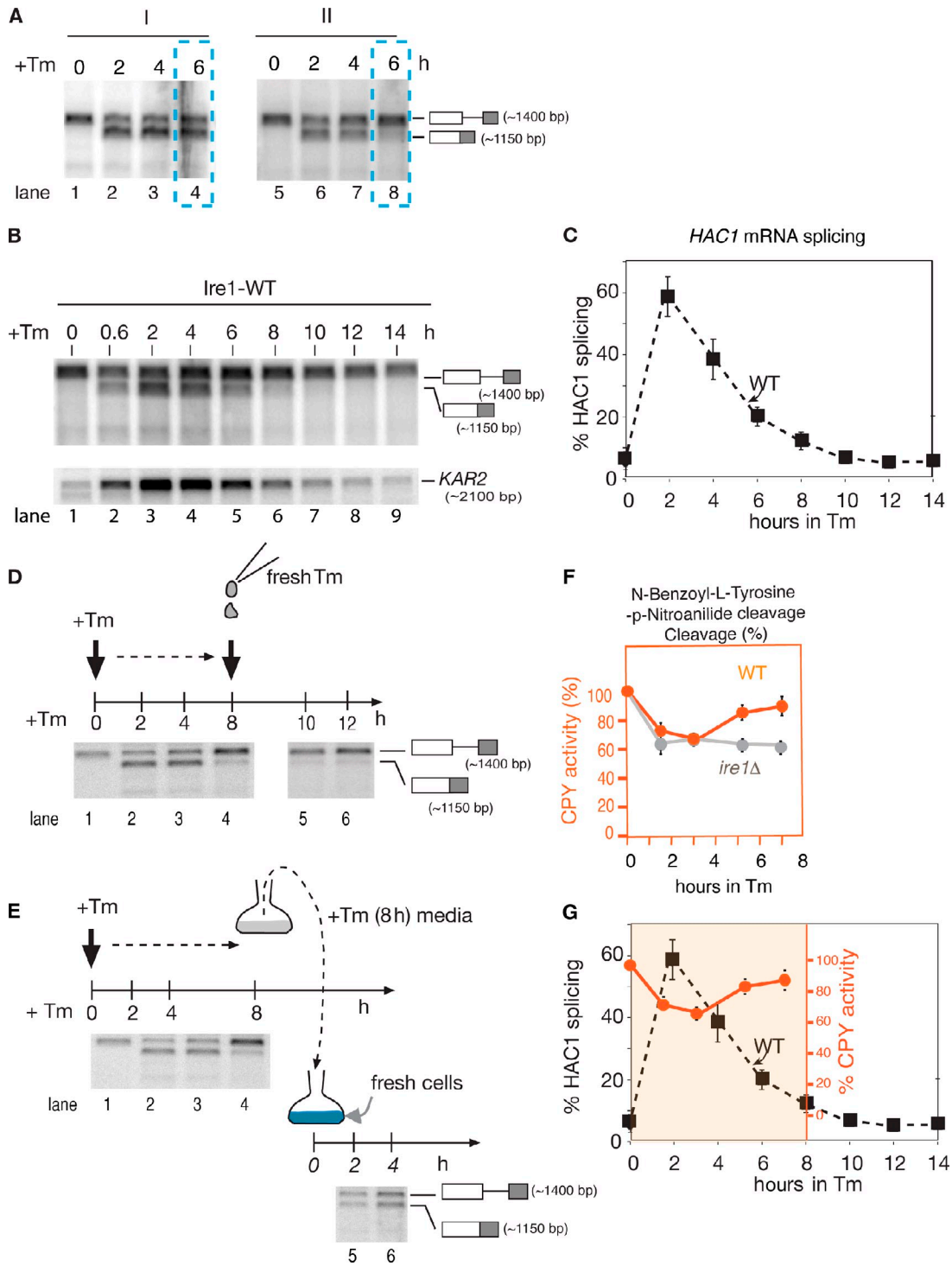www.jcb.org/cgi/doi/10.1083/jcb.201008071

JCB 41

Figure 1. **Attenuation of spliced *HAC1* mRNA levels during the UPR.** (A) *ire1Δ* yeast strain carrying WT *IRE1* (Ire1-WT) was induced for ER stress with tunicamycin (Tm) at either middle (I) or early (II) log phases. Activation of *IRE1* was monitored by *HAC1* mRNA splicing on the Northern blots of isolated RNA from cells collected at various time points. Positions of spliced and unspliced *HAC1* mRNA are indicated. Differences in HAC1 mRNA splicing are highlighted by the dotted blue boxes. (B) An extended UPR time course of Ire1-WT cells in the presence of Tm throughout the time course. The *HAC1* mRNA membrane was reprobed for *KAR2/BiP* mRNA. (C) The percentage of *HAC1* splicing (dotted line) over total *HAC1* mRNA. (D) Ire1-WT cells continuously incubated with Tm were not able to splice *HAC1* mRNA upon addition of 1 µg/ml of fresh Tm at the 8-h time point. (E) Tm in media that were incubated for 8 h was able to splice HAC1 in fresh cells that have never been treated with Tm. (F) The vacuolar carboxypeptidase Y (CPY) activity in Ire1-WT or *ire1Δ* cells with pRS341 was examined by the ability of CPY to cleave its substrate BTPNA to release *p*-nitroaniline, which was measured at 410 nm. The value of Ire1-WT cells before the UPR was set to 100% CPY activity, and the percentage of CPY activity in Ire1-WT or *ire1Δ* cells treated with Tm for the indicated lengths of time was calculated. (G) Levels of CPY activity for Ire1-WT cells were also shown (orange) and superimposed on the graph of *HAC1* mRNA splicing from C. Error bars represent standard deviations calculated from at least three independent time courses.

spliced *HAC1* mRNA was sustained for ≤6 h, suggesting that Ire1 RNase remained activated (Fig. 1, A–I). We reasoned that metabolic states of cells might affect either the activation or recovery kinetics of the UPR. Thus, we performed another UPR time course in which Tm was added to the same WT yeast cell except when they were at their earlier point of log phase. Although kinetic activation of Tm-induced *HAC1* mRNA splicing was similar to that shown in Fig. 1 (A–I), we found that most of the spliced *HAC1* mRNA disappeared after 6 h and the majority of *HAC1* mRNA was of the unspliced form (Fig. 1, A–I). A possible explanation for the disappearance of the spliced *HAC1* mRNA after 6 h may be the restoration of the ER protein-folding capacity and, thus, the termination of the UPR by inactivating Ire1 RNase. In a further extended time course (Fig. 1 B), the kinetics of appearance and the following disappearance of spliced *HAC1* mRNA correlated well with the level of *KAR2* mRNA, an immediate Hac1 transcription factor target, suggesting the potential recovery of ER protein-folding homeostasis at the later stages.

However, another explanation for decreased levels of spliced *HAC1* mRNA could be the loss of Tm activity over time. We added a second dose of fresh Tm (1 µg/ml) to the yeast culture that had already been incubated with Tm for 8 h (Fig. 1 D, lane 4, fresh Tm). Cells were no longer responsive to Tm the second time (Fig. 1 D, lanes 5 and 6), whereas the initial exposure to Tm effectively induced Ire1 (Fig. 1 D, lanes 2 and 3). Furthermore, Tm in the yeast media was still capable of activating the UPR. When Tm-containing media were taken from those grown for 8 h and added into fresh cells, *HAC1* mRNA splicing occurred efficiently (Fig. 1 E, lanes 5 and 6). In addition to the potency of Tm, these results also revealed that no "toxic" agent preventing *HAC1* mRNA splicing was secreted in the media during the initial incubation of cells with Tm. Collectively, these results suggest that decreased levels of spliced *HAC1* mRNA at later times were unlikely to be caused by a loss of the ability of Tm to induce the UPR.

Finally, we measured ER protein-folding capacity at a later time by examining the recovery of the carboxypeptidase Y (CPY) function. CPY is a vacuolar peptidase that traverses the ER, where it undergoes multiple modifications, including glycosylation, to become an enzymatically active mature form. If the later disappearance of spliced *HAC1* mRNA reflects the recovery of the ER function, glycosylation and overall folding of proteins should be restored. Thus, we monitored the CPY enzymatic activity during a Tm time course to test whether the ER protein-folding state was later recovered. CPY activity present in WT and *ire1Δ* cells that were measured by a cleavage assay using the colorimetric substrate *N*-benzoyl-L-tyrosine *p*-nitroanilide (BTPNA) in vitro (Fig. 1 F; Stevens et al., 1986; Ohi et al., 1996; Lahav et al., 2004) was decreased upon UPR induction as anticipated.

Subsequently, at 7 h, Ire1-WT cells were able to regain CPY activity at levels similar to what was present before UPR activation (Fig. 1, F and G). The recovery in CPY activity was in inverse correlation with the level of the spliced form of *HAC1* mRNA and occurred in a WT Ire1-dependent manner because CPY activity remained at low levels in *ire1Δ* UPR-deficient

cells. These results further supported the idea that the disappearance of the spliced *HAC1* mRNA reflected the recovery of ER protein-folding capacity.

Decrease in spliced *HAC1* RNA is sensitive to ER luminal information

To further test the relationship between ER functional recovery and disappearance of the spliced *HAC1* mRNA, we performed a UPR recovery assay. If disappearance of the spliced *HAC1* mRNA reflects the ER functional recovery, then removal/washing of Tm followed by incubation with fresh media should make the kinetics of the spliced *HAC1* mRNA disappearance faster. To this end, cells were washed and placed in fresh media after a 2-h Tm treatment (Fig. 2 C), and we monitored the level of spliced *HAC1* mRNA. At 2 h after Tm washout (and 4 h from the beginning of the assay), spliced *HAC1* mRNA declined by 50% (Fig. 2, C [lane 4] and D) and was mostly undetectable with the majority of *HAC1* mRNA present in the unspliced form by 3 h (Fig. 2, B, [open squares], C [lane 5], and D). The faster decline of the spliced form of *HAC1* mRNA was also observed when cells were washed after 1, 1.5, or 0.6 h of Tm treatment, at the time before reaching the maximum levels of spliced *HAC1* mRNA (Fig. 2, E–J), providing further support that the decline of spliced *HAC1* mRNA represents the recovery phase of the UPR (Fig. 2, A and B). The initial 1-h delay before the levels of spliced *HAC1* mRNA began to decline presumably reflects the time required to replenish functional glycosylation stores (Fig. 2 F), as *N*-acetylglucosamine phosphotransferase, the primary target of Tm, works at an early step in glycosylation.

Phosphomimetic mutation on the activation loop of Ire1 shows no recovery of spliced *HAC1* mRNA

Because Ire1 undergoes autophosphorylation of the activation loop during UPR induction (Shamu and Walter, 1996, Lee et al., 2008), we reasoned that its dephosphorylation might constitute at least one of the Ire1 deactivation events. We, therefore, predicted that a phosphomimetic Ire1 mutant in which three of the previously described phosphorylation sites on the activation loop (Shamu and Walter, 1996) were mutated to aspartate (Ire1-S840D/S841D/T844D) should be constitutively active or should not be able to recover once activated. Cells expressing Ire1-S840D/S841D/T844D were not constitutively active for the splicing of *HAC1* mRNA, but upon Tm addition, these cells spliced *HAC1* mRNA efficiently (Fig. 2, K and L). Thus, phosphorylation at these three residues alone is not sufficient to activate Ire1, but either phosphorylation of the fourth residue on the recently identified activation loop (Lee et al., 2008) or additional events beyond phosphorylation, such as sensing of the ER environment via the Ire1 sensor domain, must be required for activation of Ire1 (Okamura et al., 2000; Credle et al., 2005; Zhou et al., 2006; Kimata et al., 2007; Oikawa et al., 2007). Importantly, in marked contrast to WT cells, Ire1-S840D/S841D/T844D cells continued to display the spliced form of *HAC1* mRNA at later times or even after removal of Tm (Fig. 2, M–P), suggesting that dephosphorylation is required for attenuating Ire1. Collectively, the disappearance of the spliced *HAC1* mRNA
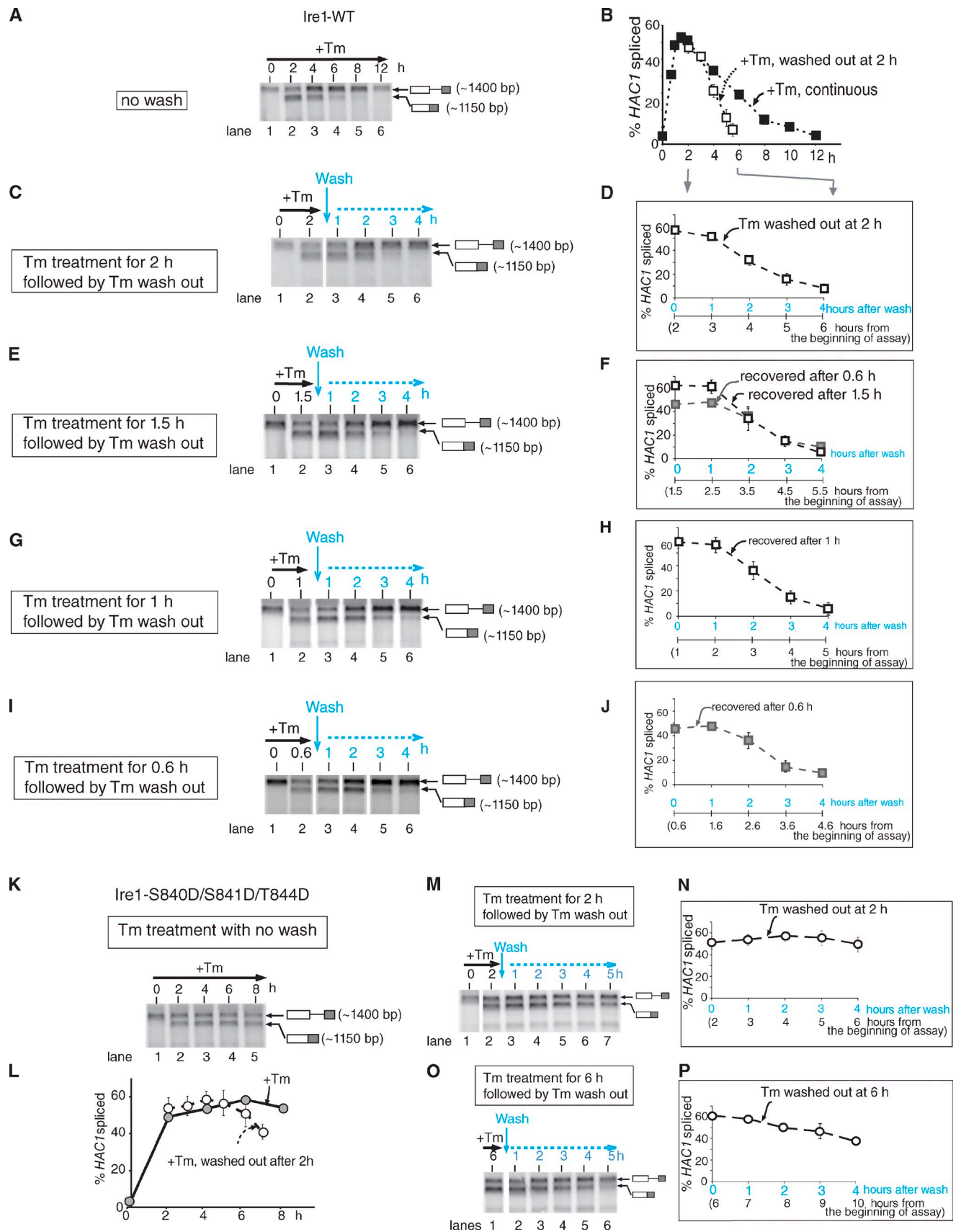
Figure 2. Removal of Tm from the medium makes the recovery of spliced *HAC1* mRNA faster in Ire1-WT cells but not in Ire1-S840D/S841D/T844D cells. (A) Ire1-WT cells incubated with Tm for the amount of time indicated. (B) Quantitation of *HAC1* mRNA splicing (closed square). (C) After a 2-h incubation with Tm, Ire1-WT cells were recovered from ER stress by washing them in warm fresh media (Wash) and incubated further without Tm for the remaining time.

at the later stage of the UPR time course reflects the reestablishment of ER protein-folding homeostasis, providing an experimental system to study the recovery phase of the UPR.

D828A Ire1 mutation causes the sustained presence of spliced *HAC1* mRNA

Using the UPR recovery assay, we examined whether any cytoplasmic domain mutants, specifically kinase domain mutants, would be defective in the transmission of the UPR attenuation signals from the ER luminal domain and display defects in decline of spliced *HAC1* mRNA upon removal of Tm. Most kinase domains, including Ire1, have critical residues that are important for ATP binding and phosphorylation. Specifically, the aspartate at 828 (D828) is within the conserved DFG kinase motif and is predicted to be involved in the coordination of β and γ phosphates of ATP with Mg^{2+} (De Bondt et al., 1993; Johnson et al., 1996; Huse and Kuriyan, 2002; Lee et al., 2008) in the kinase pocket. In an in vitro kinase assay, we found that Ire1-D828A was unable to undergo autophosphorylation despite its ability to bind to ATP, confirming that it is an inactive kinase (Fig. S1, C and D). Mutating to the alanine of this residue (Ire1-D828A) resulted in the sustained presence of spliced *HAC1* mRNA upon ER stress induction for ≤8 h. Only after that was there a gradual, small decline (Fig. 3, A and B). In parallel, the transcript of *KAR2* was also sustained at later times. The observed differences in spliced *HAC1* and *KAR2* mRNA were unlikely to be caused by the expression levels of Ire1-WT or Ire1-D828A proteins, as they were detected at similar levels (Fig. S1 A), and an increase in Ire1-D828A expression by a 2µ plasmid did not change the profile of sustained *HAC1* mRNA splicing (Fig. S1 B). Furthermore, sustained *HAC1* mRNA splicing was also observed with Ire1-D828N (unpublished data). In the recovery assay, although washing/removal of Tm and the subsequent growth in fresh media facilitated the disappearance of spliced *HAC1* mRNA in Ire1-WT cells, Ire1-D828A cells showed essentially no recovery where a spliced form of *HAC1* mRNA was persistently present, even after Tm removal. The presence of spliced *HAC1* mRNA was sustained regardless of the length of Tm treatment before removal of Tm (Fig. 3, C–J), which is similar to cells with the phosphomimetic Ire1 mutant (S840D/S841D/T844D). We also tested the involvement of the other conserved kinase domain residues, lysine at 702 (K702) and aspartate at 797 (D797), that are predicted to be important for ATP binding and phosphotransfer, respectively (De Bondt et al., 1993; Johnson et al., 1996; Huse and Kuriyan, 2002; Lee et al., 2008). However, neither of these mutants activated Ire1 RNase, making it impossible to analyze the disappearance of *HAC1* mRNA (Fig. S2). Thus, these results suggest that the Ire1 kinase domain plays an important role in terminating the UPR in addition to the activation of *HAC1* mRNA splicing.

Because phosphorylation of the activation loop is known to induce conformational changes, including movement of the loop itself, the DFG aspartate may play a role in establishing the position of the activation loop, depending on the state of ATP binding and/or autophosphorylation. Thus, D828A may allow the Ire1 RNase domain to mimic an active conformation for splicing *HAC1* mRNA, which is normally achieved by autophosphorylation of the activation loop. If this were the case, it might rescue the minimal *HAC1* mRNA-splicing levels of the Ire1-S840A/S841A/T844A activation loop mutant. Indeed, *HAC1* mRNA splicing in Ire1-D828A/S840A/S841A/T844A cells increased significantly to levels similar to that of Ire1-D828A at 2 h after UPR induction (Fig. 4 A), suggesting that the D828A mutation could convert the nonphosphorylated activation loop into a conformation suitable for RNase activation.

Finally, beyond the important phosphorylation sites on the activation loop, we reasoned that additional residues might exist to participate in such conformational changes. We inspected the presence of a conserved phenylalanine residue at position 842 (Fig. 4 B) and examined the effect of mutating F842 to alanine on *HAC1* splicing. We found that Ire1-F842A was activated to WT levels but also that, like Ire1-D828A, it showed sustained *HAC1* mRNA splicing over an extended time course (Fig. 4 C). The effect of the mutation was specific to phenylalanine at 842 as the mutation of arginine at position 843 on the activation loop to alanine had no effect on Ire1 RNase activity, demonstrating that not all Ire1 mutants with significant RNase activity result in the phenotype found in Ire1-D828A. Collectively, these results suggest that the activation loop of Ire1 is important not only during activation of Ire1 but also during the attenuation of *HAC1* mRNA splicing. In addition to simple dephosphorylation, Ire1-D828A and -F842A phenotypes have revealed the presence of another critical event for the Ire1 attenuation process.

Proper attenuation of *HAC1* splicing during UPR signaling must be important for cell physiology, although very little has been described so far. To determine the functional consequences of the sustained UPR, we examined the ability of either WT or D828A cells to grow under the UPR-induced conditions. Both WT and D828A cells grew similarly in the absence of Tm (Fig. 4 D). However, D828A cells were reduced ~25-fold in their ability to survive when grown for an extended amount of time on plates with growth medium containing 0.4 µg/ml Tm. Thus, the inability of D828A cells to attenuate *HAC1* splicing in a timely manner diminished the ability of the cells to survive the extended activation of UPR.

The white line between lanes 2 and 3 indicates the removal of intervening lanes. (D) Quantitation of *HAC1* mRNA splicing for panel C is shown. Blue numbers represent the amount of time after washing. (E–J) Cells were recovered after 1.5 (E and F)-, 1 (G and H)-, and 0.6 (I and J)-h Tm incubation, and the splicing of *HAC1* mRNA was quantified. In I, intervening lanes were spliced out between lanes 2 and 3, lanes 3 and 4, and lanes 4 and 5. (K) Ire1-S840D/S841D/T844D cells continue to retain spliced *HAC1* mRNA once activated without recovery. (L) The percentage of spliced *HAC1* mRNA (closed circle). (M–P) Ire1-S840D/S841D/T844D cells were recovered from Tm after 2 (M and N)- or 6-h (O and P) incubation, and the percentage of *HAC1* mRNA splicing was quantified. In M, the splicing of two different parts of a northern membrane is indicated by the white line between lanes 1 and 2. Error bars indicate standard deviations from at least three independent experiments.
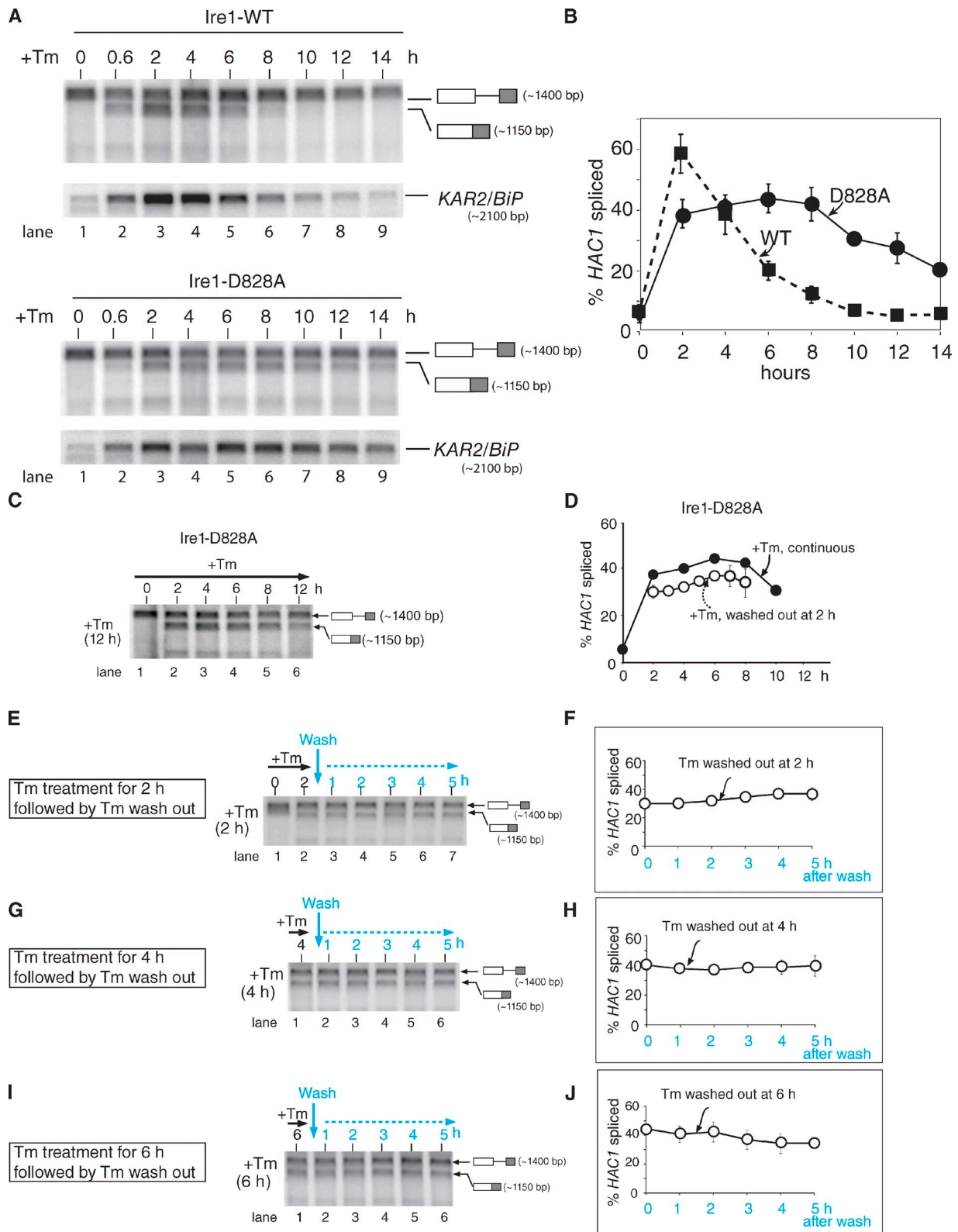
Figure 3. **Spliced *HAC1* mRNA is sustained in Ire1-D828A cells upon ER stress.** (A) Ire1-D828A cells were treated continuously with Tm for the indicated length of time for *HAC1* mRNA splicing on Northern gels and reprobed for the level of *KAR2* mRNA. As a comparison, the Tm time course of Ire1-WT cells (Fig 1B) was shown. (B) The percentage of *HAC1* mRNA spliced for Ire1-WT (closed square) and Ire1-D828A (closed circle). (C–J) Sustained presence of spliced *HAC1* RNA in Ire1-D828A cells even after the removal of Tm and resuspension in fresh media without Tm. (D) The percentage of *HAC1* mRNA splicing in cells treated with continuous Tm (closed circle) and in cells recovered after 2-h Tm treatment (open circle). (F, H, and J) Close up of the quantitation for the first 5 h of recovery. Error bars are standard deviations from at least three repeats.
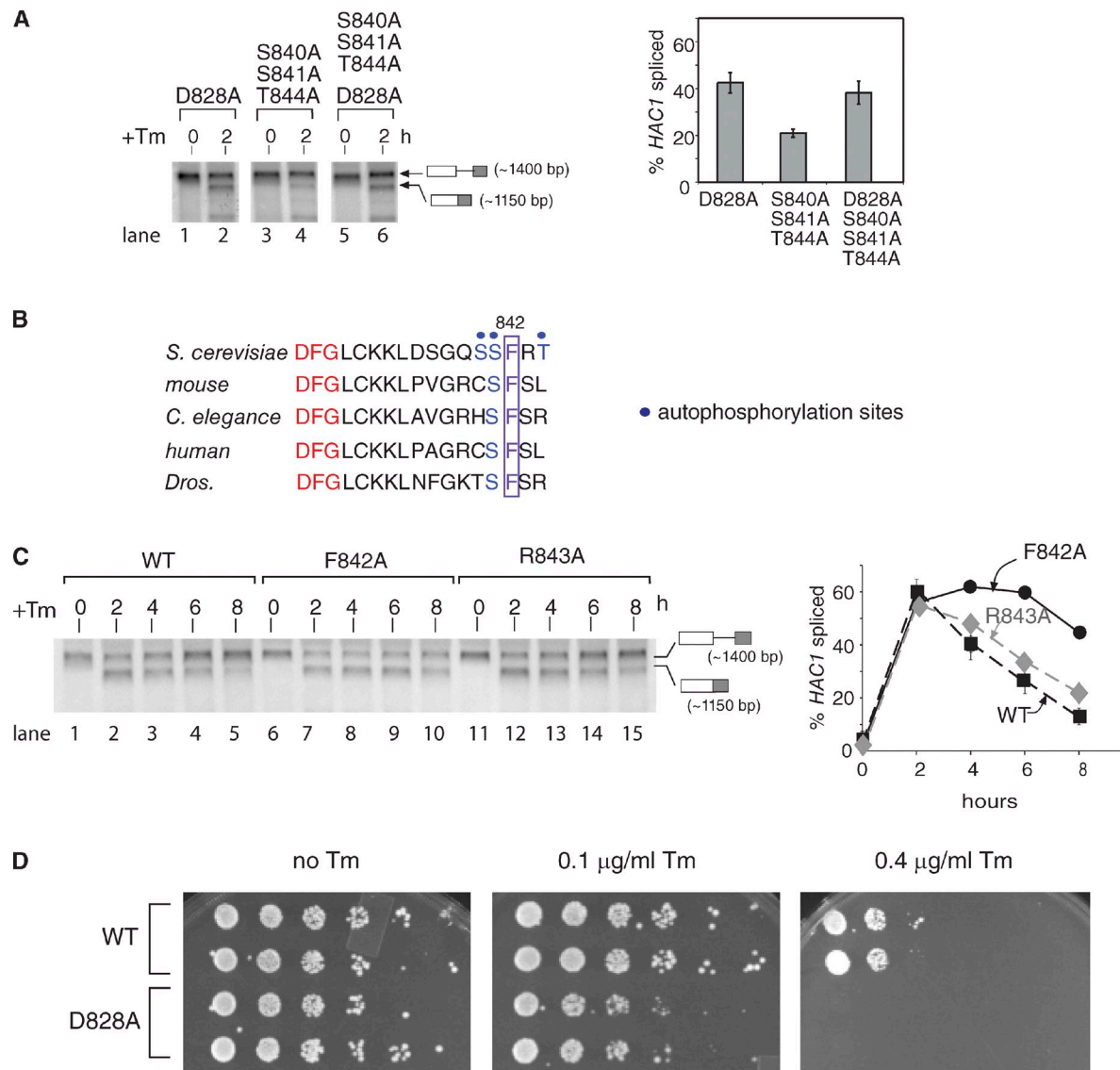
Figure 4. **An additional kinase domain mutation displays a sustained *HAC1* mRNA-splicing phenotype, and the inability to attenuate *HAC1* splicing in Ire1-D828A is more sensitive to ER stress.** (A) The D828A mutation partially rescues RNase-inactive Ire1-S840A/S841A/T844A. For each mutant, 0- and 2-h time points are shown. (B) Alignment of amino acid residues in the activation loop surrounding the DFG motif (shown in red). Serines at 840 and 841 and threonine at 844 (shown in blue) become phosphorylated upon UPR activation (Shamu and Walter, 1996; Lee et al., 2008). The conserved phenyl-alanine (F843) is shown in the purple box. (C) A mutation at the conserved phenylalanine in the activation loop (Ire1-F842A) phenocopies the Ire1-D828A mutant. (D) Ire1-D828A cells are more sensitive to ER stress. Ire1-WT or Ire1-D828A cells were grown to an OD_{600nm} of 0.25, and then cells were serially diluted by fivefold and spotted on plates containing different amounts of Tm (0, 0.1, and 0.4 µg/ml). Error bars represent standard deviations from three independent experiments. *Dros., Drosophila melanogaster.*

Although the importance of Ire1 kinase domain functions in the activation of the UPR has been demonstrated previously (Tirasophon et al., 2000; Papa et al., 2003; Lee et al., 2008), we report here that Ire1 kinase function plays an important role in the attenuation of the activated Ire1 RNase. In addition to the initial responses for the increased demands for ER functions, Ire1 must also remain sensitive to the information that ER functional capacity is reestablished to attenuate the activating signal in a timely manner. The Ire1 kinase domain plays a role in transmitting the ER luminal information to Ire1 RNase during the attenuating phase of the UPR. We have found that mutating several residues within the Ire1 kinase domain, D828, F842, S8440, S841, and T844, resulted in an essentially similar

phenotype of cells becoming insensitive to the reestablishment of the ER functional capacity and having the sustained presence of the spliced *HAC1* mRNA. This was in contrast to WT cells in which removal of Tm, an ER stress agent, facilitated the disappearance of the spliced *HAC1* mRNA. The importance of the timely attenuation of the UPR was supported by the inability of Ire1-D828A cells to sustain their growth, even though these cells are able to mount *HAC1* mRNA splicing at the initial phase.

One interesting finding is that mutations in multiple different residues of the Ire1 kinase domain showed similar phenotypes of the sustained presence of the spliced *HAC1* mRNA. Simultaneously, in addition to the mutants we report here, a new study independently shows that another kinase-inactive

mutant Ire1 (D797N or K799N) is unable to attenuate Ire1 RNase (see Rubio et al. in this issue). As these residues are also projected toward the kinase catalytic cleft, they may provide the framework for conformational changes needed for attenuating Ire1 RNase activity. For example, the involvement of the DFG motif in a more direct catalytic function beyond nucleotide binding (Johnson et al., 1996; Huse and Kuriyan, 2002) has been predicted from structural studies with insulin receptor kinase (IRK) and Src and Abl kinases (Till et al., 2001; Levinson et al., 2006). The ability of the DFG motif to affect activation loop conformation is also supported by the finding that the D828A mutation converts the nonphosphorylatable activation loop mutant (Ire1-S840A/S841A/T844A) into an active RNase (Fig. 4 A).

Conversely, in IRK (Till et al., 2001), alteration of the IRK activation loop residue (IRK-D1161A) induced a structural disorder in the IRK nucleotide-binding pocket, mimicking a transition state. Similarly, the conserved activation loop phenylalanine (F842) on the Ire1 activation loop may be involved in the establishment of certain critical hydrophobic interactions that allow a unique conformational link with the nucleotide-binding pocket. Thus, a specific conformational link between the residues within the nucleotide binding and the activation loop, including the DFG motif and phosphorylation sites, may provide the molecular bases for using the evolutionarily conserved kinase domain for both activation and attenuating signals in response to changes in the luminal domain of Ire1.

Several signaling pathways use multiple strategies for signal attenuation (Dikic and Giordano, 2003). In mammalian cells, a recent study has shown that the spliced form of XBP1 mRNA goes away after 12 h of a Tm incubation time course (Lin et al., 2007). In contrast, other UPR inducers, such as PERK or ATF6, remain active for a while, suggesting that Ire1 was inactivated even before the ER capacity recovery. In addition to the splicing of XBP1 mRNA, however, the UPR in

mammalian cells appears to be negatively regulated by the XBP1 protein coded from the unspliced form of XBP1 mRNA (pXBP1(U); Yoshida et al., 2006). As pXBP1(U) concentration increases at later times, heterodimer formation with a spliced form (pXBP1(S)) causes pXBP1(S) to be transported to the cytoplasm where it undergoes proteasome-mediated degradation. Such a mechanism may allow the cell to inactivate the transcriptional response even before the inactivation of Ire1. In yeast, although no evidence for the production of pHAC1(U), presumably caused by the presence of the translational inhibitory intron within unspliced *HAC1*, is found, other negative factors generated during the UPR may facilitate UPR down-regulation.

Human diseases that correlate with insufficient UPR activation are rapidly increasing. For example, the loss of pancreatic β cells in juvenile diabetic patients (Wolcott–Rallison syndrome) is thought to be caused by the loss of the functional PERK protein, another ER transmembrane kinase involved in UPR induction (Harding et al., 2001). Our finding that Ire1 can be trapped in an activated state for an extended length of time by modulation of the kinase domain may provide a basis for the development of novel strategies for augmenting UPR insufficiency in some human diseases.

Materials and methods

Yeast strains and plasmids
Yeast strains carrying various forms of *IRE1* were generated by the standard yeast transformation protocol (Elble, 1992). Mutant forms of *IRE1* were generated using the QuickChange kit (Agilent Technologies) and confirmed by sequencing the entire coding region. Tables I and II summarize the yeast strains and plasmids used in this study. The KAR2 plasmid was a gift from D. Ng (National University of Singapore, Singapore).

Cell culture and growth conditions
All yeast strains were grown in synthetic complete media supplemented with inositol at a final concentration of 50 µg/ml. Tm (EMD) was added to

Table I. **Yeast strains used in this study**

Strain	Genotype	Source/reference
MNY1000	MATα; ura3-1; leu2-3-112; his3-11-15; trp1-1; ade2-1; can1-100	Cox et al., 1993
MNY1013	Same as MNY1000 except ire1::URA3	Cox et al., 1993
MNY1014	Same as MNY1013 with pRS314	This study
MNY1015	Same as MNY1013 with pCS110	This study
MNY1016	Same as MNY1013 with pMHR001	This study
MNY1017	Same as MNY1013 with pMHR002	This study
MNY1018	Same as MNY1013 with pMHR003	This study
MNY1019	Same as MNY1017 with pMR713	This study
MNY1020	Same as MNY1017 with pRS315	This study
MNY1021	Same as MNY1015 with pRS315	This study
MNY1022	Same as MNY1013 with pCS122	This study
MNY1023	Same as MNY1013 with pMHR004	This study
MNY1024	Same as MNY1015 with pMR713	This study
MNY1025	Same as MNY1013 with pMHR005	This study
MNY1026	Same as MNY1013 with pMHR006	This study
MNY1027	Same as MNY1013 with pMHR007	This study
MNY1028	Same as MNY1013 with pMHR008	This study
MNY1029	Same as MNY1013 with pMHR010	This study
MNY1030	Same as MNY1013 with pMHR011	This study

a final concentration of 1 µg/ml to induce the UPR when required. Yeast strains were grown overnight to saturation with an OD_{600} of ~1.5. The following morning, cells were diluted to 0.75–0.8 × 10^7 cells/ml and allowed to recover for one doubling time in fresh media to reach an OD_{600} of ~0.5. Upon addition of Tm, cells were collected for analysis of RNA at the time points indicated in the figures.

Isolation of RNA and Northern blot analyses
Total RNA was isolated according to the hot phenol method (Köhrer and Domdey, 1991). RNA was separated by electrophoresis on 1.5% agarose gels containing 6.7% formaldehyde and transferred to a Duralon-UV membrane (Agilent Technologies) as previously described (Cox and Walter, 1996). Hybridization was performed at 65°C overnight in church buffer containing 0.5 M Na_2HPO_4, 1 mM EDTA, and 7% SDS, pH 7.5. Quantitation of Northern blots was performed on an imager system (Typhoon 9400; GE Healthcare). All probes were labeled with α-[^{32}P]deoxy-CTP using a DNA-labeling system (Megaprime; GE Healthcare). The probe used for detecting both spliced and unspliced forms of *HAC1* mRNA was as described previously (Papa et al., 2003). The *KAR2* probe was generated by PCR of a 0.5-kb fragment of the coding region. The percentage of *HAC1* splicing was calculated as the percentage of spliced over total *HAC1* mRNA.

CPY functional assay
CPY catalyzed the hydrolysis of its substrate BTPNA (Sigma-Aldrich) to give the yellow product *p*-nitroaniline, whose production was followed by an increase in absorbance at 410 nm. Cells were permeabilized in a buffer containing 100 mM Tris, pH 7.6, and 0.2% Triton X-100 for 30 min at 37°C in the presence of BTPNA. Upon permeabilization, the BTPNA gained access to mature vacuolar CPY for the cleavage reaction, which was measured by absorbance value in 410 nm. The absorbance value obtained from UPR-uninduced cells was set to 100%, and the percentage of functional CPY activity was calculated.

Recombinant Ire1 protein expression and in vitro kinase assay
The GST-tagged WT Ire1-(linker kinase tail [LKT])p containing the entire cytosolic domain of Ire1 (aa 556–1,115) was expressed and purified as described previously (Sidrauski and Walter, 1997). The fusion protein was purified using glutathione–Sepharose beads (GE Healthcare). All the mutant forms of Ire1 were prepared essentially in a similar manner. In vitro autophosphorylation of various forms of the recombinant Ire1p was performed as described previously (Nock et al., 2001). In brief, the recombinant Ire1 was incubated in kinase buffer (10 mM Hepes, pH 7.5, 5 mM Mg(OAc)$_2$, 25 mM KOAc, and 1 mM DTT) containing 200 µM of unlabeled ATP and 167 µCi γ-[^{32}P]ATP (7,000 Ci/mmol; ICN) at 30°C for 30 min before being analyzed on 7% SDS-PAGE. Levels of various forms of the recombinant Ire1 proteins were examined by staining the gel with SYPRO ruby staining based on the manufacturer's instructions (Invitrogen).

Yeast protein extract and Western blot analyses
Pellets from cells with an OD_{600} of 3 were resuspended in 100 µl SUME (1% SDS, 8 M urea, 10 mM MOPS, pH 6.8, and 10 mM EDTA) with protease inhibitors (1 mM PMSF, 10 µg/ml tosyl phenylalanyl chloromethyl ketone, leupeptin, and pepstatin). The total cell extract was prepared by vortexing in the presence of 100 µl of 0.5-mm acid-washed glass beads at 4°C. 100 µl of 2× USB (75 mM MOPS, pH 6.8, 4% SDS, 200 mM DTT, and 8 M urea) was then added, and the samples were incubated at 65°C for 10 min. Proteins were isolated on SDS-PAGE and were transferred on to a nitrocellulose membrane, which was probed for either Ire1-WT or Ire1-D828A using an anti-HA antibody (Santa Cruz Biotechnology, Inc.).

Fluorescent nucleotide-binding assay
An increasing amount (5–120 µM) of the fluorescent nucleotides *N*-methylanthraniloyl nucleotide (MANT)-ADP and MANT-ATP (Invitrogen) were mixed with 1.4 µM recombinant Ire1(LKT) in 25 mM Tris, pH 7.5, 0.4 M NaCl, 5% glycerol, and 10 mM MgCl$_2$ before being excited at 280 nm. The emission was measured at 440 nm using a spectrofluorometer (Fluoromax; Horiba Scientific) as described previously in detail (Ni et al., 2000). The equilibrium dissociation constants were determined by plotting the changes in fluorescence at 440 nm as a function of nucleotide concentration (either MANT-ATP or MANT-ADP, 5–120 µM) and are the concentrations of a MANT nucleotide at which 50% of the maximum fluorescence changes was measured as described previously (Adams and Taylor, 1992; Ni et al., 2000).

Online supplemental material
Fig. S1 shows that Ire1-D828A is expressed and binds ATP at a level similar to Ire1-WT but is an inactive kinase. Fig. S2 shows that nucleotide binding and phosphorylation are important for the full activation of Ire1 RNase. Online supplemental material is available at http://www.jcb.org/cgi/content/full/jcb.201008071/DC1.

Table II. **Plasmids used in this study**

Plasmid	Description	Backbone	Source/reference
pCS110	WT *IRE1* gene (Trp)	pRS314 (cen/ars)	Cox et al., 1993
pCS122	WT *IRE1* gene (Trp)	yEPLac112 (2µ)	Shamu and Walter, 1996
pMR713	WT *KAR2* gene (Leu)	pRS315 (cen/ars)	Ng et al, 2000
pMHR001	K702A mutation in *IRE1*	pCS110	This study
pMHR002	D828A mutation in *IRE1*	pCS110	This study
pMHR003	S840A/S841A/T844A mutations in *IRE1*	pCS110	This study
pMHR004	D828A mutation in *IRE1*	pCS122	This study
pMHR005	S840D/S841D/T844D mutations in *IRE1*	pCS110	This study
pCF210	*Escherichia coli* expression plasmid for GST-*IRE1* (aa 556–1,115)	pGEX-6P-2	Sidrauski and Walter, 1997
pMHR006	D797A mutation in Ire1	pCS110	This study
pMHR007	R843A mutation in Ire1	pCS110	This study
pMHR008	F842A mutation in Ire1	pCS110	This study
pMHR009	*E. coli* expression plasmid for His-*IRE1* (aa 642–1,115)	pET15b	This study
pMHR010	D828A/S840A/S841A/T844A mutations in *IRE1*	pCS110	This study
pMHR011	D828N mutation in *IRE1*	pCS110	This study
pMHR012	*E. coli* expression plasmid for His-*IRE1* (aa 642–1,111) with D828A	pMHR009	This study

cen/ars, centromeric/autonomously replicating sequence.

References

Adams, J.A., and S.S. Taylor. 1992. Energetic limits of phosphotransfer in the catalytic subunit of cAMP-dependent protein kinase as measured by viscosity experiments. *Biochemistry*. 31:8516–8522. doi:10.1021/bi00151a019

Aragón, T., E. van Anken, D. Pincus, I.M. Serafimova, A.V. Korennykh, C.A. Rubio, and P. Walter. 2009. Messenger RNA targeting to endoplasmic reticulum stress signalling sites. *Nature*. 457:736–740. doi:10.1038/nature07641

Cox, J.S., and P. Walter. 1996. A novel mechanism for regulating activity of a transcription factor that controls the unfolded protein response. *Cell*. 87:391–404. doi:10.1016/S0092-8674(00)81360-4

Cox, J.S., C.E. Shamu, and P. Walter. 1993. Transcriptional induction of genes encoding endoplasmic reticulum resident proteins requires a transmembrane protein kinase. *Cell*. 73:1197–1206. doi:10.1016/0092-8674(93)90648-A

Credle, J.J., J.S. Finer-Moore, F.R. Papa, R.M. Stroud, and P. Walter. 2005. On the mechanism of sensing unfolded protein in the endoplasmic reticulum. *Proc. Natl. Acad. Sci. USA*. 102:18773–18784. doi:10.1073/pnas.0509487102

De Bondt, H.L., J. Rosenblatt, J. Jancarik, H.D. Jones, D.O. Morgan, and S.-H. Kim. 1993. Crystal structure of cyclin-dependent kinase 2. *Nature*. 363:595–602. doi:10.1038/363595a0

Dikic, I., and S. Giordano. 2003. Negative receptor signalling. *Curr. Opin. Cell Biol.* 15:128–135. doi:10.1016/S0955-0674(03)00004-8

Elble, R. 1992. A simple and efficient procedure for transformation of yeasts. *Biotechniques*. 13:18–20.

Harding, H.P., and D. Ron. 2002. Endoplasmic reticulum stress and the development of diabetes: a review. *Diabetes*. 51(Suppl. 3):S455–S461. doi:10.2337/diabetes.51.2007.S455

Harding, H.P., H.Q. Zeng, Y.H. Zhang, R. Jungries, P. Chung, H. Plesken, D.D. Sabatini, and D. Ron. 2001. Diabetes mellitus and exocrine pancreatic dysfunction in perk−/− mice reveals a role for translational control in secretory cell survival. *Mol. Cell*. 7:1153–1163. doi:10.1016/S1097-2765(01)00264-7

Huse, M., and J. Kuriyan. 2002. The conformational plasticity of protein kinases. *Cell*. 109:275–282. doi:10.1016/S0092-8674(02)00741-9

Johnson, L.N., M.E.M. Noble, and D.J. Owen. 1996. Active and inactive protein kinases: structural basis for regulation. *Cell*. 85:149–158. doi:10.1016/S0092-8674(00)81092-2

Kaufman, R.J. 1999. Stress signaling from the lumen of the endoplasmic reticulum: coordination of gene transcriptional and translational controls. *Genes Dev.* 13:1211–1233. doi:10.1101/gad.13.10.1211

Kawahara, T., H. Yanagi, T. Yura, and K. Mori. 1997. Endoplasmic reticulum stress-induced mRNA splicing permits synthesis of transcription factor Hac1p/Ern4p that activates the unfolded protein response. *Mol. Biol. Cell*. 8:1845–1862.

Kawahara, T., H. Yanagi, T. Yura, and K. Mori. 1998. Unconventional splicing of HAC1/ERN4 mRNA required for the unfolded protein response. Sequence-specific and non-sequential cleavage of the splice sites. *J. Biol. Chem.* 273:1802–1807. doi:10.1074/jbc.273.3.1802

Kimata, Y., Y. Ishiwata-Kimata, T. Ito, A. Hirata, T. Suzuki, D. Oikawa, M. Takeuchi, and K. Kohno. 2007. Two regulatory steps of ER-stress sensor Ire1 involving its cluster formation and interaction with unfolded proteins. *J. Cell Biol.* 179:75–86. doi:10.1083/jcb.200704166

Köhrer, K., and H. Domdey. 1991. Preparation of high molecular weight RNA. *Methods Enzymol.* 194:398–405.

Lahav, R., A. Nejidat, and A. Abeliovich. 2004. Alterations in protein synthesis and levels of heat shock 70 proteins in response to salt stress of the halotolerant yeast *Rhodotorula mucilaginosa*. *Antonie van Leeuwenhoek*. 85:259–269. doi:10.1023/B:ANTO.0000020361.81006.2b

Lee, K.P.K., M. Dey, D. Neculai, C. Cao, T.E. Dever, and F. Sicheri. 2008. Structure of the dual enzyme Ire1 reveals the basis for catalysis and regulation in nonconventional RNA splicing. *Cell*. 132:89–100. doi:10.1016/j.cell.2007.10.057

Levinson, N.M., O. Kuchment, K. Shen, M.A. Young, M. Koldobskiy, M. Karplus, P.A. Cole, and J. Kuriyan. 2006. A Src-like inactive conformation in the abl tyrosine kinase domain. *PLoS Biol.* 4:e144. doi:10.1371/journal.pbio.0040144

Lin, J.H., H. Li, D. Yasumura, H.R. Cohen, C. Zhang, B. Panning, K.M. Shokat, M.M. Lavail, and P. Walter. 2007. IRE1 signaling affects cell fate during the unfolded protein response. *Science*. 318:944–949. doi:10.1126/science.1146361

Mori, K. 2000. Tripartite management of unfolded proteins in the endoplasmic reticulum. *Cell*. 101:451–454. doi:10.1016/S0092-8674(00)80855-7

Mori, K., W. Ma, M.J. Gething, and J. Sambrook. 1993. A transmembrane protein with a cdc2+/CDC28-related kinase activity is required for signaling from the ER to the nucleus. *Cell*. 74:743–756. doi:10.1016/0092-8674(93)90521-Q

Ng, D.T.W., E.D. Spear, and P. Walter. 2000. The unfolded protein response regulates multiple aspects of secretory and membrane protein biogenesis and endoplasmic reticulum quality control. *J. Cell Biol.* 150:77–88. doi:10.1083/jcb.150.1.77

Ni, Q., J. Shaffer, and J.A. Adams. 2000. Insights into nucleotide binding in protein kinase A using fluorescent adenosine derivatives. *Protein Sci.* 9:1818–1827. doi:10.1110/ps.9.9.1818

Nock, S., T.N. Gonzalez, C. Sidrauski, M. Niwa, and P. Walter. 2001. Purification and activity assays of the catalytic domains of the kinase/endoribonuclease Ire1p from *Saccharomyces cerevisiae*. *Methods Enzymol.* 342:3–10. doi:10.1016/S0076-6879(01)42530-4

Ohi, H., W. Ohtani, N. Okazaki, N. Furuhata, and T. Ohmura. 1996. Cloning and characterization of the *Pichia pastoris* PRC1 gene encoding carboxypeptidase Y. *Yeast*. 12:31–40. doi:10.1002/(SICI)1097-0061(199601)12:1<31::AID-YEA877>3.0.CO;2-S

Oikawa, D., Y. Kimata, and K. Kohno. 2007. Self-association and BiP dissociation are not sufficient for activation of the ER stress sensor Ire1. *J. Cell Sci.* 120:1681–1688. doi:10.1242/jcs.002808

Okamura, K., Y. Kimata, H. Higashio, A. Tsuru, and K. Kohno. 2000. Dissociation of Kar2p/BiP from an ER sensory molecule, Ire1p, triggers the unfolded protein response in yeast. *Biochem. Biophys. Res. Commun.* 279:445–450. doi:10.1006/bbrc.2000.3987

Papa, F.R., C. Zhang, K. Shokat, and P. Walter. 2003. Bypassing a kinase activity with an ATP-competitive drug. *Science*. 302:1533–1537. doi:10.1126/science.1090031

Patil, C., and P. Walter. 2001. Intracellular signaling from the endoplasmic reticulum to the nucleus: the unfolded protein response in yeast and mammals. *Curr. Opin. Cell Biol.* 13:349–355. doi:10.1016/S0955-0674(00)00219-2

Ron, D., and P. Walter. 2007. Signal integration in the endoplasmic reticulum unfolded protein response. *Nat. Rev. Mol. Cell Biol.* 8:519–529. doi:10.1038/nrm2199

Rubio, C.A., D. Pincus, A.V. Korennykh, S. Schuck, H. El-Samad, and P. Walter. 2011. Homeostatic adaptation to endoplasmic reticulum stress depends on Ire1 kinase activity. *J. Cell Biol.* 193:171–184.

Rüegsegger, U., J.H. Leber, and P. Walter. 2001. Block of HAC1 mRNA translation by long-range base pairing is released by cytoplasmic splicing upon induction of the unfolded protein response. *Cell*. 107:103–114. doi:10.1016/S0092-8674(01)00505-0

Shamu, C.E., and P. Walter. 1996. Oligomerization and phosphorylation of the Ire1p kinase during intracellular signaling from the endoplasmic reticulum to the nucleus. *EMBO J.* 15:3028–3039.

Sidrauski, C., and P. Walter. 1997. The transmembrane kinase Ire1p is a site-specific endonuclease that initiates mRNA splicing in the unfolded protein response. *Cell*. 90:1031–1039. doi:10.1016/S0092-8674(00)80369-4

Stevens, T.H., J.H. Rothman, G.S. Payne, and R. Schekman. 1986. Gene dosage-dependent secretion of yeast vacuolar carboxypeptidase Y. *J. Cell Biol.* 102:1551–1557. doi:10.1083/jcb.102.5.1551

Till, J.H., A.J. Ablooglu, M. Frankel, S.M. Bishop, R.A. Kohanski, and S.R. Hubbard. 2001. Crystallographic and solution studies of an activation loop mutant of the insulin receptor tyrosine kinase: insights into kinase mechanism. *J. Biol. Chem.* 276:10049–10055. doi:10.1074/jbc.M010161200

Tirasophon, W., K. Lee, B. Callaghan, A. Welihinda, and R.J. Kaufman. 2000. The endoribonuclease activity of mammalian IRE1 autoregulates its mRNA and is required for the unfolded protein response. *Genes Dev.* 14:2725–2736. doi:10.1101/gad.839400

Travers, K.J., C.K. Patil, L. Wodicka, D.J. Lockhart, J.S. Weissman, and P. Walter. 2000. Functional and genomic analyses reveal an essential coordination between the unfolded protein response and ER-associated degradation. *Cell*. 101:249–258. doi:10.1016/S0092-8674(00)80835-1

Wickner, W., and R. Schekman. 2005. Protein translocation across biological membranes. *Science*. 310:1452–1456. doi:10.1126/science.1113752

Yoshida, H., M. Oku, M. Suzuki, and K. Mori. 2006. pXBP1(U) encoded in XBP1 pre-mRNA negatively regulates unfolded protein response activator pXBP1(S) in mammalian ER stress response. *J. Cell Biol.* 172:565–575. doi:10.1083/jcb.200508145

Zhou, J., C.Y. Liu, S.H. Back, R.L. Clark, D. Peisach, Z. Xu, and R.J. Kaufman. 2006. The crystal structure of human IRE1 luminal domain reveals a conserved dimerization interface required for activation of the unfolded protein response. *Proc. Natl. Acad. Sci. USA*. 103:14343–14348. doi:10.1073/pnas.0606480103